Copy No. 107

[redacted]

RM No. L8F04

c1

NACA

RESEARCH MEMORANDUM

EFFECT OF GROUND INTERFERENCE ON THE AERODYNAMIC CHARACTERISTICS OF A 42° SWEPTBACK WING

By

G. Chester Furlong and Thomas V. Bollech

Langley Aeronautical Laboratory
Langley Field, Va.

NATIONAL ADVISORY COMMITTEE FOR AERONAUTICS

WASHINGTON
September 7, 1948

[redacted]

9/10/48

 [redacted]

NATIONAL ADVISORY COMMITTEE FOR AERONAUTICS

RESEARCH MEMORANDUM

EFFECT OF GROUND INTERFERENCE ON THE AERODYNAMIC CHARACTERISTICS OF A 42° SWEPTBACK WING

By G. Chester Furlong and Thomas V. Bóllech

SUMMARY

The effects of ground interference on the aerodynamic characteristics of a 42° sweptback wing have been investigated at distances 0.68 and 0.92 of the mean aerodynamic chord above the ground. The wing was tested without flaps and with inboard trailing-edge split flaps and outboard leading-edge flaps deflected.

The nature and magnitudes of the ground interference effects on the aerodynamic characteristics of the sweptback wing are, in general, comparable to those obtained on unswept wings. The sweptback wing in the presence of the ground sustained an increase in lift-curve slope and a decrease in drag. The value of maximum lift for the sweptback wing increased for the flaps-retracted configuration and decreased for the flaps-deflected configurations as the distance from the ground became smaller.

The longitudinal stability at the stall for the sweptback wing with and without flaps deflected was not materially affected by the presence of the ground. There was, however, at the smallest distance from the ground a destabilizing change in pitching-moment slope at an angle of attack several degrees lower than the stalling angle of attack for the flaps-deflected configuration. Because of the complexity of the phenomenon at the stall, the possibility exists that the present data on a sweptback wing are not indicative of the type of stability to be obtained at distances from the ground greater than the mean aerodynamic chord of the wing.

INTRODUCTION

Certain aspects of the effects of the ground interference on the aerodynamic characteristics of unswept wings have been thoroughly investigated both theoretically and experimentally (references 1 to 6). The experimental results of these investigations have shown that, in the high-lift range, theoretical calculations by existing methods do not provide either an estimate of the magnitude of the ground effects or an explanation of the phenomena involved at the stall.

[redacted]

Inasmuch as extensions of theoretical calculations into the high-lift range are not reliable and the available experimental data in the high-lift range are confined to wings having little or no sweepback, it appears that a knowledge of the effects of the ground on a highly sweptback wing can only be acquired by means of experiment. Accordingly, an investigation has been conducted in the Langley 19-foot pressure tunnel to determine the effects of ground interference on a highly sweptback wing and to indicate whether the ground effects on a sweptback wing are of the same general nature and magnitude as those on an unswept wing.

The model used for the present investigation had 42° sweepback of the leading edge, an aspect ratio of 4, a taper ratio of 0.625, and NACA 64_1-112 airfoil sections normal to the 0.273 chord line.

Tests were made with and without a simulated ground for two model configurations; namely, the plain wing and the wing with trailing-edge split flaps and outboard leading-edge flaps deflected. Force and moment data were obtained throughout the angle-of-attack range and at several values of Reynolds numbers.

The ground was simulated in the tunnel by means of a ground board. Although this method of ground representation is not ideal, the results of the present tests are believed to be indicative of the effects of ground interference on a sweptback wing.

SYMBOLS

C_L	lift coefficient $\left(\frac{\text{Lift}}{qS}\right)$
C_D	drag coefficient $\left(\frac{\text{Drag}}{qS}\right)$
C_m	pitching-moment coefficient about $0.25\bar{c}$ $\left(\frac{\text{Pitching moment}}{qS\bar{c}}\right)$
α	angle of attack, degrees
R	Reynolds number $\left(\frac{\rho V\bar{c}}{\mu}\right)$
q	dynamic pressure $\left(\frac{\rho V^2}{2}\right)$, pounds per square foot
S	wing area, square feet
b	wing span, feet
c	wing chord, feet
ρ	mass density of air, slugs per cubic foot

μ coefficient of viscosity of air, slugs per foot-second

V stream velocity, feet per second

$\bar{c}$ mean aerodynamic chord $\left(\frac{2}{S}\int_0^{b/2} c^2\,dy\right)$, feet

y spanwise distance, feet

GROUND, MODEL, AND APPARATUS

Ground Representation and Ground Distance

Several methods such as the reflection method, the partial plate and reflection method, and the plate method are available for ground simulation in a wind tunnel (references 4 to 6). The most feasible arrangement for ground tests in the Langley 19-foot pressure tunnel is the plate method (commonly referred to as the ground-board method).

The vertical distance from the $0.25\bar{c}$ to the ground board (regardless of boundary-layer thickness on the ground board) is referred to as the ground distance. Inasmuch as no standard point of reference exists, the $0.25\bar{c}$ has been used because it is the most convenient point of reference from considerations of test procedure. The model is supported in the tunnel at the $0.25\bar{c}$, and to maintain a constant ground distance for any other point of reference would have necessitated moving the ground board as the angle of attack of the wing was changed.

Based on the preceding definition of ground distance, the ground distances used in the present tests were $0.68\bar{c}$ and $0.92\bar{c}$.

Model

The model mounted on the normal wing-support system of the Langley 19-foot pressure tunnel is shown in figure 1. The wing had 42° sweepback of the leading edge, a taper ratio of 0.625, an aspect ratio of 4.01, and NACA 64_1-112 airfoil sections normal to the 0.273 chord line. The 0.20c trailing-edge split flaps were deflected 60° from the lower surface and extended from the root to $0.50\frac{b}{2}$. The leading-edge flaps extended from $0.400\frac{b}{2}$ to $0.975\frac{b}{2}$. The principal dimensions of the model and flaps are given in figure 2.

Prior to the present investigation, the wing had been equipped with a leading-edge slat which extended from $0.400 \frac{b}{2}$ to $0.975 \frac{b}{2}$. In the retracted position the slat was found to alter slightly the NACA 64_1-112 airfoil sections and to cause a slight discontinuity along the 0.20 chord line. The aerodynamic characteristics obtained in the present test, therefore, do not necessarily represent exactly those which would be obtained on a wing with true NACA 64_1-112 airfoil sections. The model was maintained in a smooth condition during the tests.

APPARATUS

The ground board used in the investigation is shown schematically in figure 3 and consisted of a steel framework covered with plywood on both the upper and lower surfaces. The over-all thickness of the ground board was 4 inches. The ground board was fitted with a round leading edge and a tapered trailing edge. A boundary-layer control slot, which was perpendicular to the longitudinal center line of the tunnel, extended the full width of the board. The slot was located 1 foot in front of the $0.25\bar{c}$ of the wing so that the root and tip sections of the wing were in front of and behind the slot, respectively. Air flow through the slot was obtained by means of a lower-surface flap which was used to provide a pressure differential between the upper and lower surface of the ground board. The ground board was supported in the tunnel test section by means of wall brackets and center posts (figs. 1 and 3). The support system allowed a ground-board travel from 16 to 31.9 inches below the center line of the tunnel (center of rotation of the model).

The aerodynamic forces and moments were measured by a simultaneously recording, 6-component balance system.

TESTS AND CORRECTIONS

Tests

The air in the tunnel was compressed to an absolute pressure of approximately 33 pounds per square inch for all tests.

Exploratory tests.- An exploratory investigation was conducted to determine the flow characteristics on the ground board and in the tunnel test section both with and without the model in the tunnel.

The change in velocity distribution in the tunnel due to the ground board was determined with the ground board in the tunnel and the model out. Measurements of the flow beneath the board indicated that the increase in flow due to the presence of the model was hardly measurable; hence the usual model blockage correction has been applied to the dynamic pressure measurements. The ground board reduced the tunnel-clear stream angle approximately 0.15°.

Visual tuft studies of the flow on the ground board with the boundary-layer slot closed and open were made through the angle-of-attack range of the model. When the slot was closed but not completely sealed, an unsteady flow condition existed along the nose of the slot. The flow condition at the nose of the slot was improved when the slot was open. An unsteady flow condition existed in an area near the center of the board between $2.0\bar{c}$ and $2.8\bar{c}$ (location shown in fig. 3) with either the slot open or closed. This unsteady flow condition can be attributed to the diffusion of the flap wake. There was no indication of actual flow separation on the board throughout the angle-of-attack range of the model. By use of the boundary-layer control slot the maximum thickness of the boundary layer was reduced from approximately 1.0 inch to 0.4 inch beneath the wing and from 1.6 inches to 1.0 inch at a distance $2.8\bar{c}$ rearward of the $0.25\bar{c}$. The flow through the slot was not materially affected by the presence of the model. The discontinuity in boundary-layer thickness due to the flow through the slot corresponds to an effective discontinuity in ground distance, which, however, is believed to have a negligible effect on the test results. Presence of a boundary layer on the ground board may be less troublesome under a sweptback wing than under an unswept wing, mainly because the maximum lift is considerably lower for the sweptback wing.

Force and moment tests.- Force and moment data were obtained for the two model configurations through an angle-of-attack range from -4° through the stall. The tests were made with the ground board out and with the ground board located at ground distances of $0.68\bar{c}$ and $0.92\bar{c}$ for several values of Reynolds number. The Reynolds numbers of the tests were 3.0, 4.3, 5.2, and 6.8×10^6 based on the mean aerodynamic chord of the wing. A Reynolds number of 6.8×10^6 corresponds to a dynamic pressure of approximately 80 pounds per square foot and a Mach number of 0.16.

Corrections

Ground board out.- The lift, drag, and pitching-moment data have been corrected for support tare and strut interference as determined from tare tests. The angles of attack, drag data, and moment data have been corrected for jet-boundary effects. In addition, the angles of attack have been corrected for air-stream misalinement.

Ground board in.- With the ground board in the tunnel test section, no corrections could be obtained for support tare and strut interference. The ground-board out corrections for support tare and strut interference, however, have been applied to the ground-board-in data in the belief that they would be of the same nature, although not necessarily of the same magnitude, as would be obtained with the ground board in.

Calculations made for other ground investigations (such as reference 4) have shown that at small ground distances jet-boundary corrections are negligible; hence, they have been neglected in the present tests.

PRELIMINARY DISCUSSION OF EFFECTS OF GROUND INTERFERENCE

A discussion of the concepts of ground interference appears pertinent before the results of the present tests of a sweptback wing are presented. Although the concepts have been derived largely to explain the effects of ground interference on an unswept wing, they should, in general, apply to a sweptback wing as well.

The ground effect on a wing may be considered as the interference due to the reflected image of the wing in the ground. Computations of the effects of the image wing on the real wing can be made by replacing it with a bound vortex and a system of trailing vortices. Inasmuch as these computations are based on thin-wing theory, the effect of the thickness of the image wing must also be determined. The separate effects of the bound vortex, trailing vortices, and wing thickness can then be added. In reference 1 the interference from the trailing vortices of the image wing was considered in detail; whereas in reference 6 the interferences from the bound vortex and wing thickness of the image wing were also considered. Although the calculations of the separate interference effects for unswept wings have been shown experimentally to be inadequate in the high angle-of-attack range, the separate effects may be used to describe qualitatively the combined effects of angle of attack and ground distance.

The image trailing vortices induce an upwash at the wing which is stronger at the center than near the tips. Figure 4(a) shows the trailing vortices of the wing and its image. The main effects shown are an increase in lift-curve slope, a reduction in induced drag, and a concentration of lift toward the center of the wing. The effects are increased by decreasing the ground distance and are relatively independent of the angle of attack.

The induced flow over the wing due to the image bound vortex is shown by a side view of the wing and its image (fig. 4(b)). The flow, which is from rear to front, reduces the stream velocity in the vicinity of the wing and thereby tends to reduce the lift. If, however, the wing is fairly close to the ground, is at a moderate angle of attack, and is uncambered, the induced flow also has a vertical component near the rear (fig. 4(b)) which corresponds to an effective increase in camber and a corresponding increase in lift. As either the angle of attack or the camber is increased, however, the induced flow crosses the wing from above (as in fig. 4(c)) with a corresponding effective decrease in camber and reduction in lift. For a highly cambered airfoil, such as a flapped wing, this effect is very pronounced. The decrease in camber and reduction in lift as the angle of attack is increased is also a function of ground distance. As the ground distance becomes very small, the effects mentioned are delayed to higher and higher angles of attack.

The thickness of the image wing may be roughly represented by a source near the airfoil nose and an equivalent sink near its trailing edge. The corresponding streamlines are circles through the source and sink, as indicated in figures 4(d) and 4(e). The velocity is in such a direction as to increase the stream velocity in the vicinity of the wing. The induced flow is seen to be (figs. 4(d) and 4(e)) essentially independent of angle of attack and is downward near the trailing edge and upward at the nose. This induced flow corresponds to a negative induced camber and a reduction in lift. The induced-flow effect of the doublet is increased as the ground distance is reduced, but in any case this effect is small compared with the induced-flow effect of the bound vortex (figs. 4(b) and 4(c)).

In general, at low angles of attack and low lift coefficients the induced flows indicated in figures 4(a), 4(b), 4(d), and 4(e) serve to increase the slope of the lift curve. As the angle of attack and lift coefficient become very large or when the flaps are deflected, the induced flow indicated in figure 4(c) becomes increasingly strong and serves to reduce the lift-curve slope. The over-all influence of these effects on the maximum lift is too complex to be explained without a more quantitative analysis.

Experimental results provide some indication of the important factors determining the maximum lift as the ground is approached. Data for straight, unflapped wings (references 1 and 6) show that the maximum lift is decreased and then increased as the ground is approached. The reduced stream velocity and the negative induced angle and camber indicated in figure 4(c) appear to combine with the small induced flow of figure 4(e) to effect a decrease in maximum lift at moderate ground distances. As previously mentioned the negative induced angle and camber effect (fig. 4(c)) is reduced appreciably for uncambered wings as the ground distance becomes small; hence the maximum lift begins to increase. The experimental data for straight, flapped wings (reference 4) show a decrease in maximum lift at all ground distances down to $0.50\bar{c}$. In this case the wing is originally very highly cambered and the negative induced angle and camber indicated in figure 4(c) are not materially decreased by a decrease in ground distance.

For sweptback wings most of the effects just described would probably remain the same. With regard to the spanwise distribution of loading, however, calculations made as a part of the present investigation have indicated that, when the effect of the swept bound vortices is included with the effect indicated in figure 4(a) (calculated in reference 1), the induced upwash distribution should tend to concentrate the loading near the tips instead of near the center. This effect, combined with the fact that the tip sections of a sweptback wing are much closer to the ground than the root sections, would be expected to result in a noticeable outboard shift in load. The tip stall usually associated with sweptback wings might be increased in severity by such an outboard shift in load.

RESULTS AND DISCUSSION

The lift, drag, and pitching-moment data are presented in figures 5 and 6. The stalling characteristics are presented in figures 7 and 8.

The greater part of the present discussion is in reference to the data obtained at a Reynolds number of 6.8 million.

Lift-Curve Slope

The slope of the lift curve near $C_L = 0$, for the wing with and without flaps, increased as the distance to the ground decreased (figs 5(a) and 6(a)). The increase is, in general, comparable to the increase obtained for an unswept wing without flaps (reference 4). The data do not indicate a shift in angle of zero lift. Such a shift is indicated by the theory and test data for an unswept wing presented in reference 6. No such shift, however, was indicated by the unswept-wing data of reference 4. The reduction in lift-curve slope attributable to ground interference in the high angle-of-attack range was much more severe for the flaps-deflected configuration (fig. 6(a)) than for the flaps-retracted configuration (fig. 5(a)).

Maximum Lift

The data of figure 5(a) for the wing without flaps show an increasing maximum lift coefficient at the ground distances of the present tests (less than $1.0\bar{c}$). The data of the present tests do not extend to sufficiently high ground distances to show whether a sweptback wing will sustain a loss in maximum lift when first entering the presence of the ground. Both the magnitude of the increase in maximum lift and the magnitude of the ground distances at which the increase in lift is obtained appear to be greater than the magnitudes obtained for unswept wings (references 4 and 6). It should be remembered, however, that the points of reference used to determine the ground distances for a sweptback wing and an unswept wing are not directly comparable.

The data for the sweptback wing with flaps deflected (fig. 6(a)) show an appreciable loss in maximum lift at the same ground distances at which increases in maximum lift were obtained for the flaps-retracted configuration (fig. 5(a)). The decrease in maximum lift at small ground distances is in general accordance with the results obtained on unswept wings with flaps deflected (reference 4).

Drag

A reduction in drag (figs. 5(b) and 6(b)) was obtained when both model configurations were tested in the presence of the ground board. Throughout the comparable lift range the model with flaps deflected encountered slightly larger decreases in drag than were encountered with the flaps-retracted configuration. The reductions in drag are, in general, comparable with the reductions obtained for unswept wings (reference 4).

Stalling Patterns

The results of the visual stall observations (figs. 7 and 8) show that for the flaps-deflected model configuration the presence of the ground precipitated a stall on the upper surface of the wing at a slightly lower angle of attack. Stall studies with the ground board out are not available for the wing without flaps after the installation of the leading-edge slat. The stall studies indicate that, in general, the origin and progression of the stall are little affected by the presence of the ground.

Pitching Moment

The presence of the ground did not materially affect the longitudinal stability at the stall for either model configuration of the sweptback wing. The plain wing remained unstable (fig. 5(c)) at the stall and the wing with flaps deflected remained stable (fig. 6(c)). At the lowest ground distance ($0.68\bar{c}$) a noticeable destabilizing change in pitching-moment slope several degrees prior to the stalling angle was obtained for the flaps-deflected configuration. These effects are similar to those reported for an unswept wing (reference 4).

It appears from the present data that at the ground distances of the present tests the outboard shift in load that might be expected with a sweptback wing is effectively counterbalanced by the increase in effective camber and by a reduction in adverse pressure gradients at the tip sections. The net result is that the origin and progression of the stall are little affected by the presence of the ground and hence the stability at the stall is not changed. The possibility of severe tip stalling and accompanying instability at the stall for the sweptback wing at ground distances greater than those of the present tests could not be ascertained and remains a problem to be investigated.

Scale Effects

For the flaps-retracted configuration there appears to be some scale effect on the lift in the high-lift and stalling region. Because of this effect the stabilizing change in pitching-moment slope obtained at a lift coefficient of 0.8 for a Reynolds number of 3.0×10^6 is delayed to a lift coefficient of approximately 1.0 at a Reynolds number of 6.8 million (fig. 5(c)). The slight improvement in the stability at the stall which is obtained for the smallest ground distance and a Reynolds number of 3.0×10^6 is not obtained at a Reynolds number of 6.8×10^6.

The effects of Reynolds number on the lift, drag, and pitching-moments for the wing with flaps deflected appear to be small.

CONCLUDING REMARKS

An investigation has been conducted to determine the ground interference effects on the aerodynamic characteristics of a 42° sweptback wing. The simulated ground tests were made at ground distances 0.68 and 0.92 of the mean aerodynamic chord. The model was tested without flaps and with inboard trailing-edge split flaps and outboard leading-edge flaps deflected. The results of the tests indicated:

1. The nature and magnitudes of the effects of ground interference on the aerodynamic characteristics of the sweptback wing are, in general, comparable to those obtained on unswept wings. The sweptback wing in the presence of the ground board sustained an increase in lift-curve slope and a decrease in drag. The value of maximum lift for the sweptback wing increased for the flaps-retracted configuration and decreased for the flaps-deflected configuration as the distance from the ground became smaller.

2. The longitudinal stability at the stall for the sweptback wing with and without flaps deflected was not materially affected by the presence of the ground. There was, however, at the lowest distance from the ground a destabilizing change in pitching-moment slope several degrees prior to the stall for the flaps-deflected configuration. Because of the complexity of the phenomenon at the stall, the possibility exists that the present data on a sweptback wing are not indicative of the type of

stability to be obtained at ground distances greater than one mean aerodynamic chord.

Langley Aeronautical Laboratory
National Advisory Committee for Aeronautics
Langley Field, Va.

REFERENCES

1. Wieselsberger, C.: Wing Resistance near the Ground. NACA TM No. 77, 1922.

2. Pistolesi, E.: Ground Effect – Theory and Practice. NACA TM No. 828, 1937.

3. Reid, Elliot G.: A Full-Scale Investigation of Ground Effect. NACA Rep. No. 265, 1927.

4. Recant, Isidore G.: Wind-Tunnel Investigation of Ground Effect on Wings with Flaps. NACA TN No. 705, 1939.

5. Katzoff, S., and Sweberg, Harold H.: Ground Effect on Downwash Angles and Wake Location. NACA Rep. No. 738, 1943.

6. Tani, Itiro, Taima, Masuo, and Simidu, Sodi: The Effect of Ground on the Aerodynamic Characteristics of a Monoplane Wing. Rep. No. 156 (vol. XIII, 2), Aero. Res. Inst., Tokyo Imperial Univ., Sept. 1937.

L8622

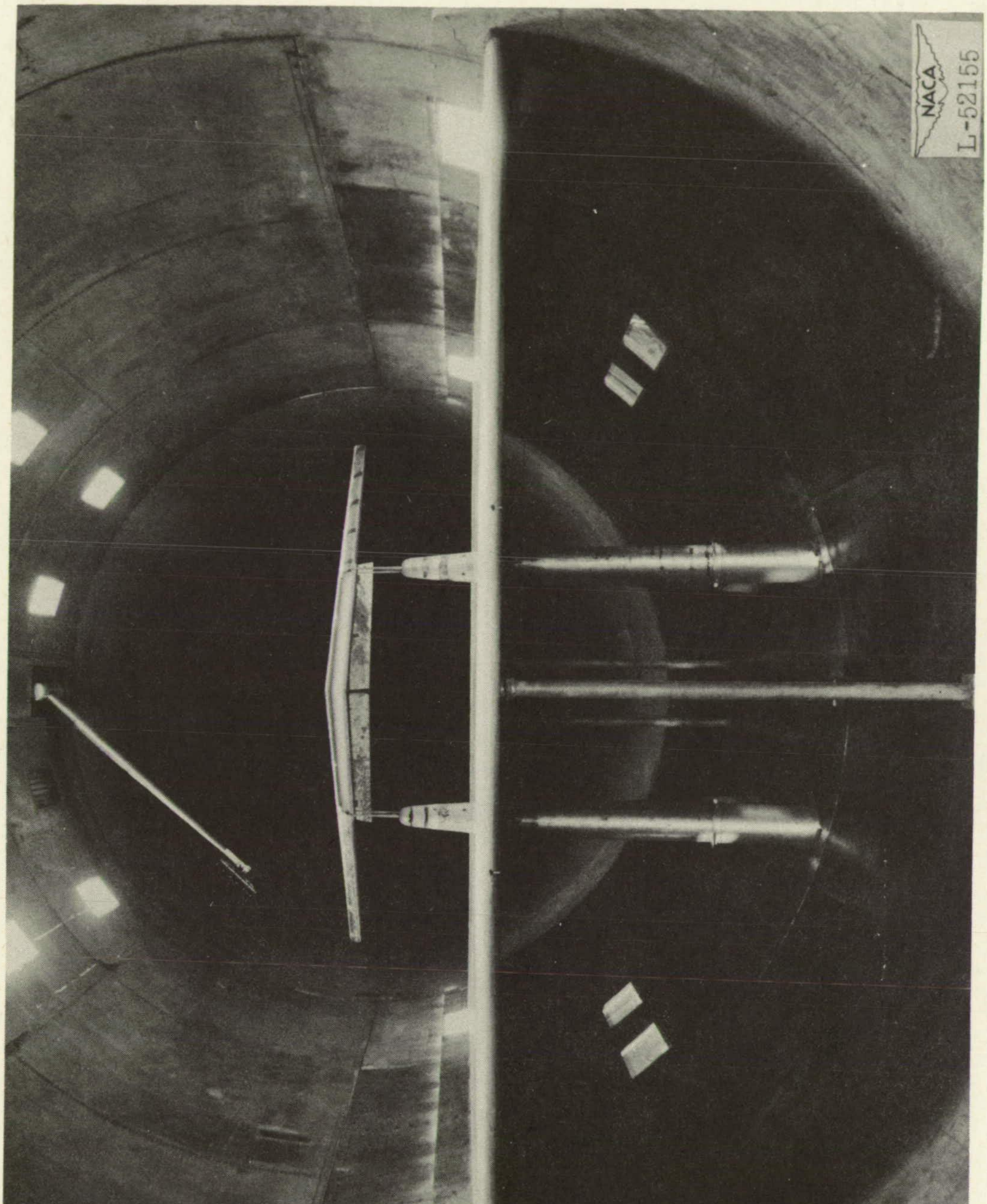

(a) Front view.

Figure 1.- The 42° sweptback wing mounted in the Langley 19-foot pressure tunnel. Flaps deflected; ground board in. Ground distance $0.92\bar{c}$.

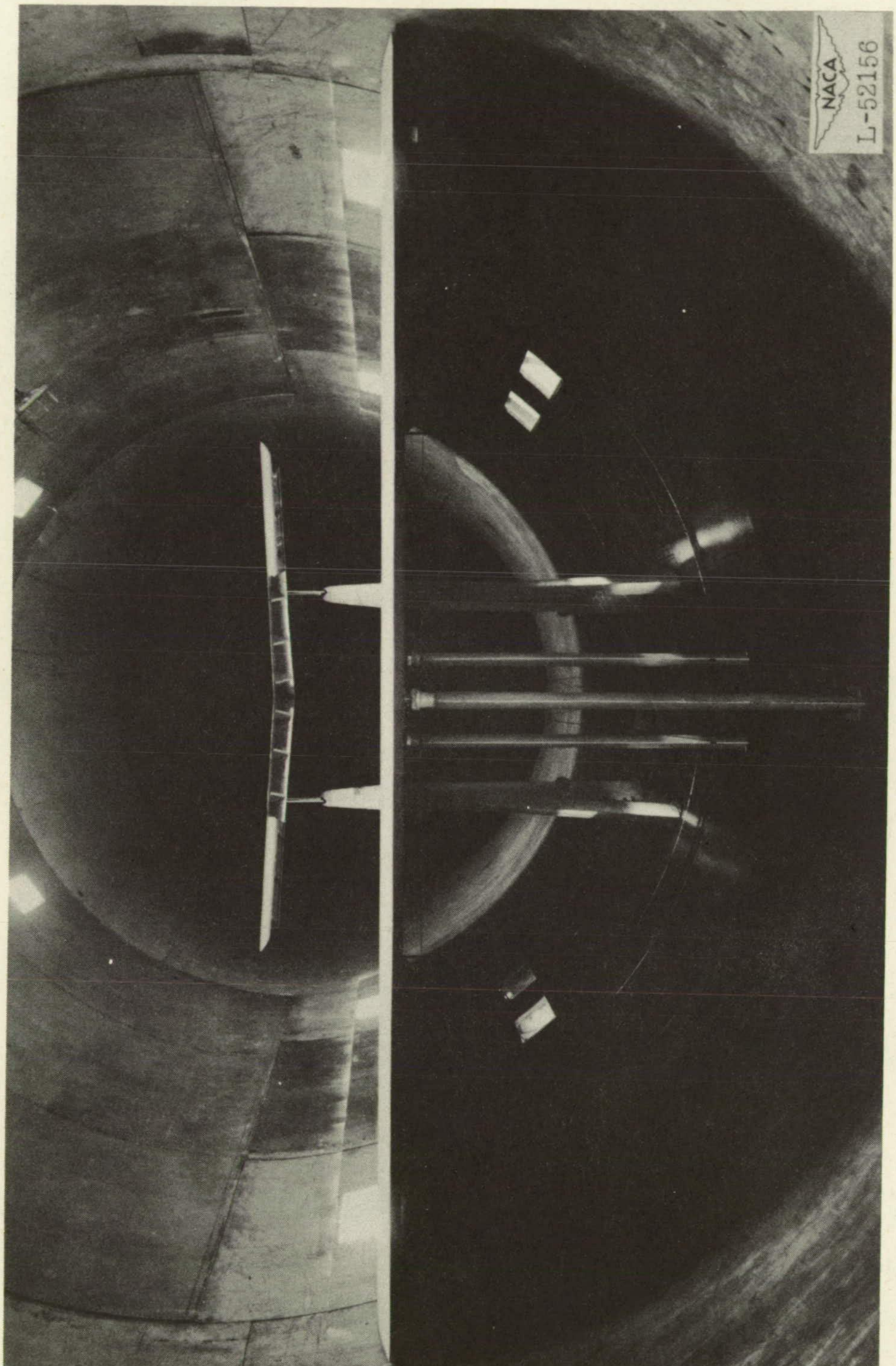

(b) Rear view.

Figure 1.- Concluded.

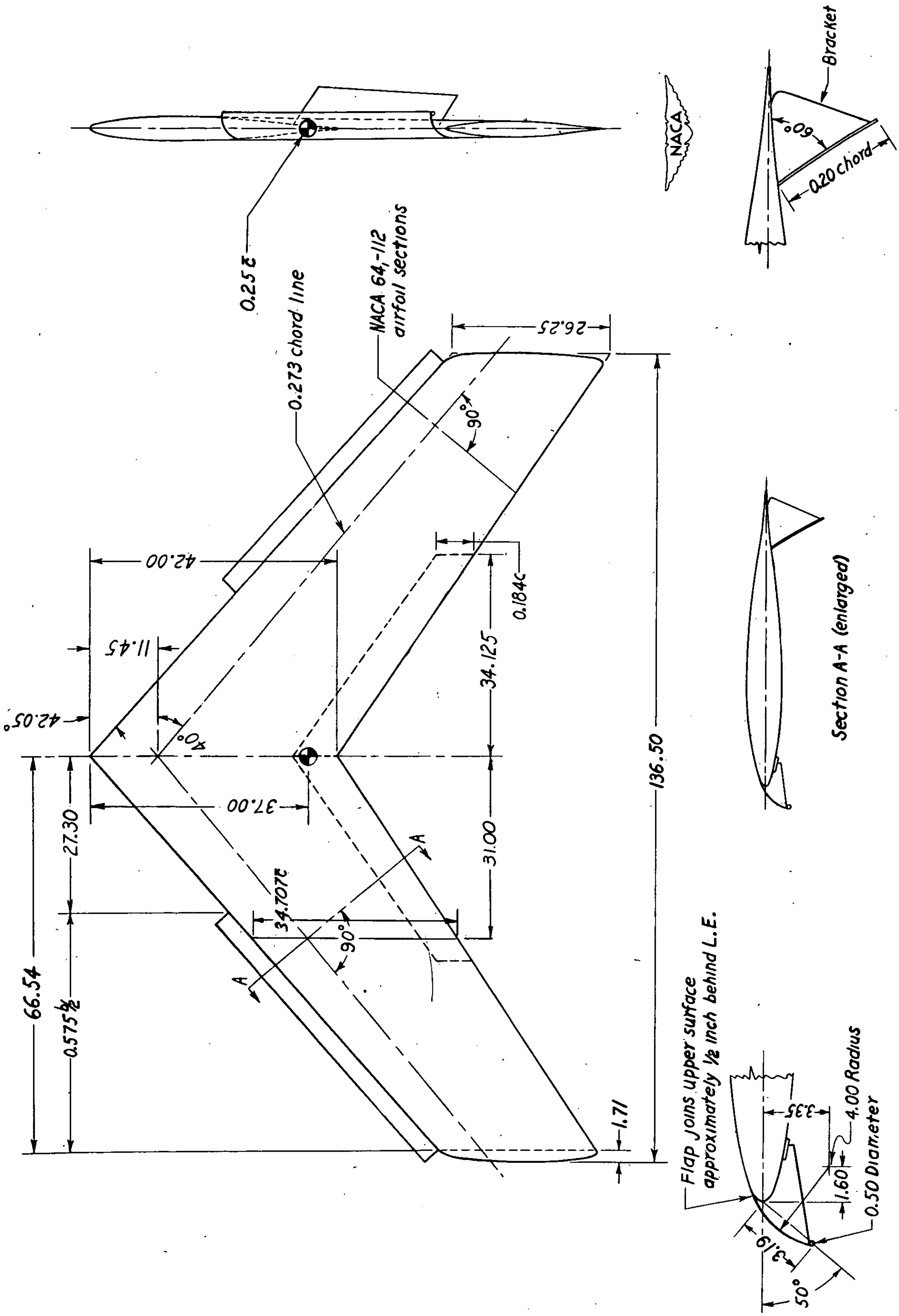

Figure 2.- Layout of 42° sweptback wing. (All dimensions are in inches.)

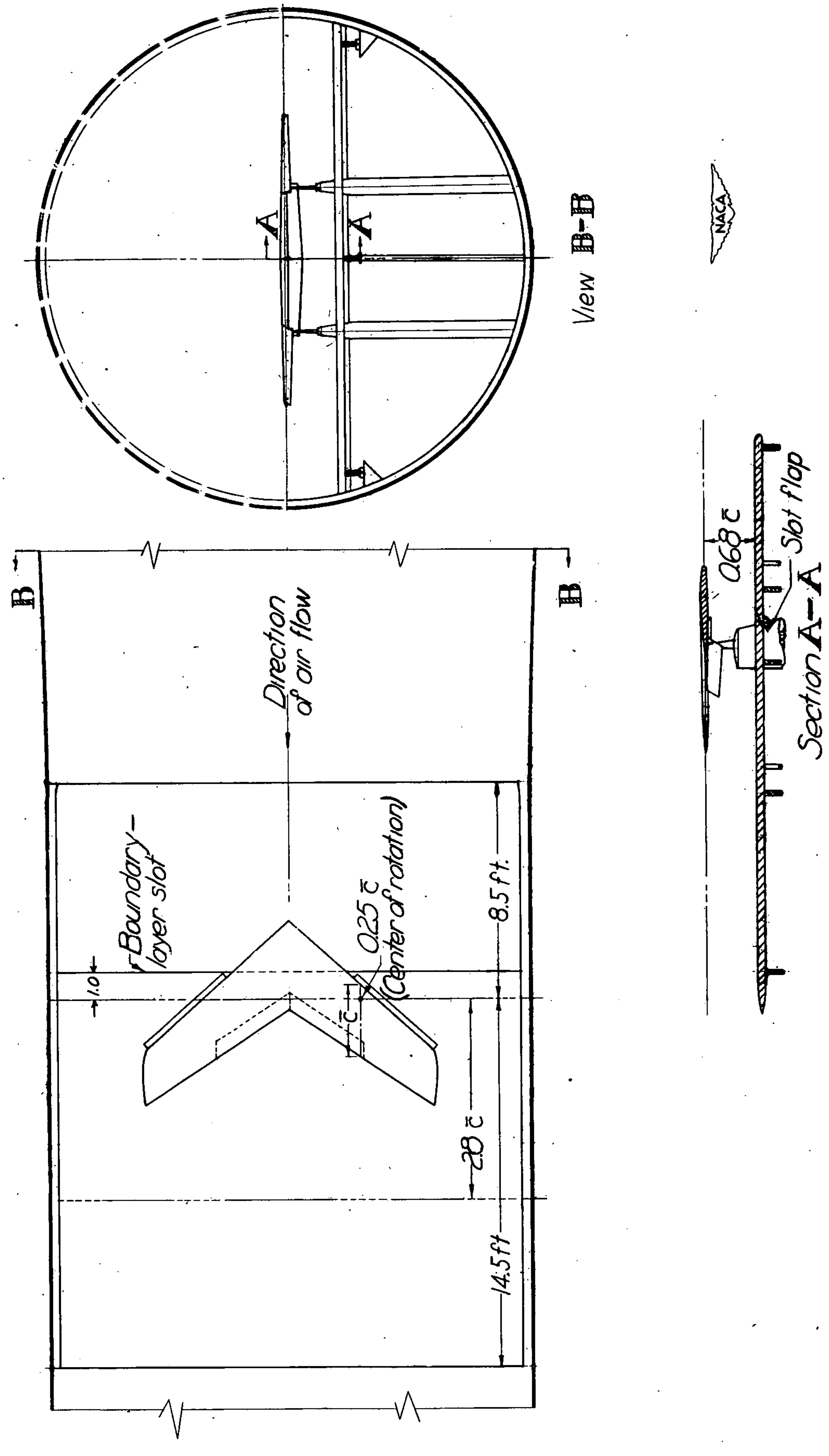

Figure 3.- Sketch of 42° sweptback wing and ground board used in the 19-foot pressure tunnel. Ground distance 0.68c̄.

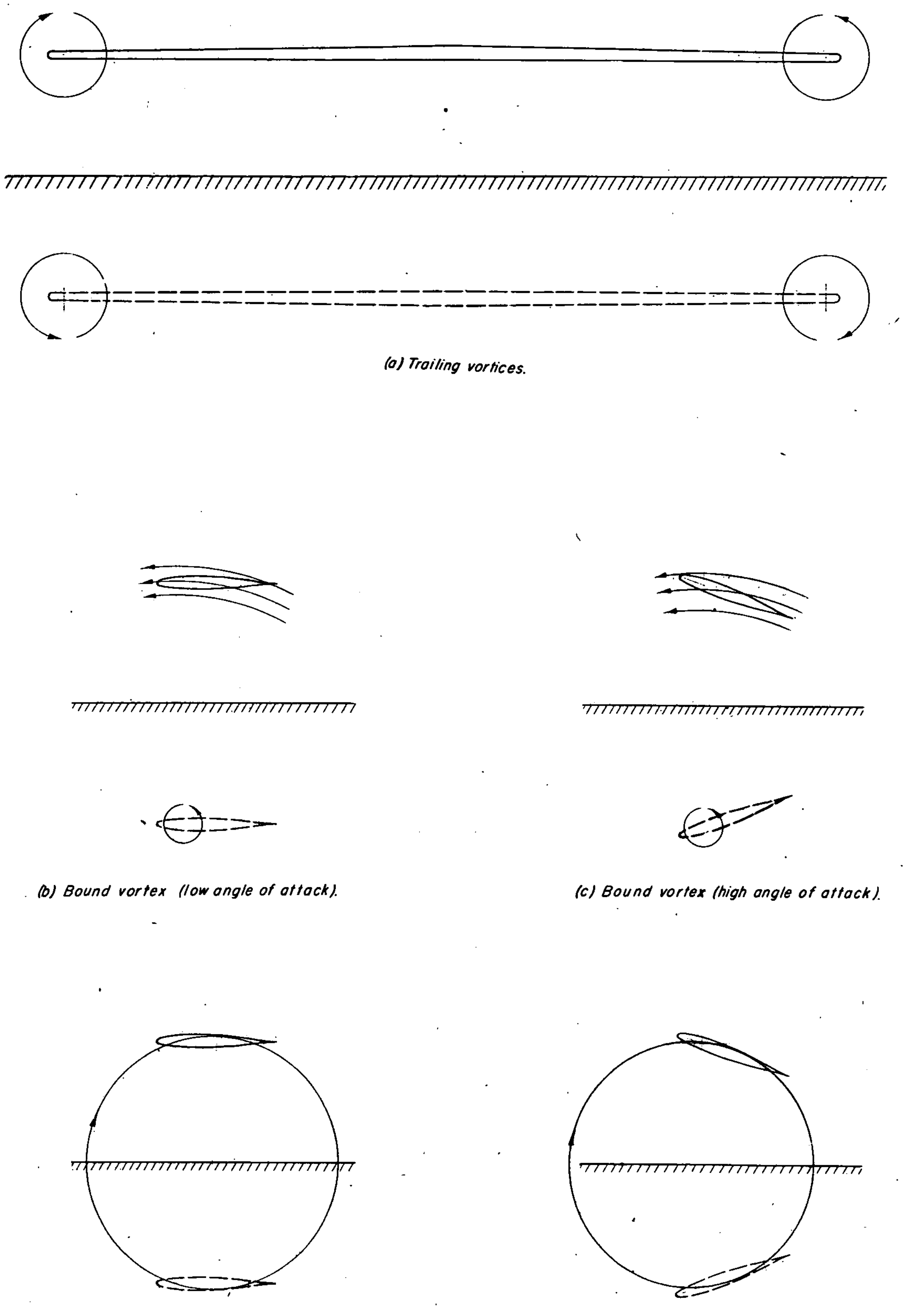

(a) Trailing vortices.

(b) Bound vortex (low angle of attack).

(c) Bound vortex (high angle of attack).

(d) Wing thickness doublet (low angle of attack).

(e) Wing thickness doublet (high angle of attack).

Figure 4.- Sketch showing the interference effects of the reflected image of a wing in the presence of the ground.

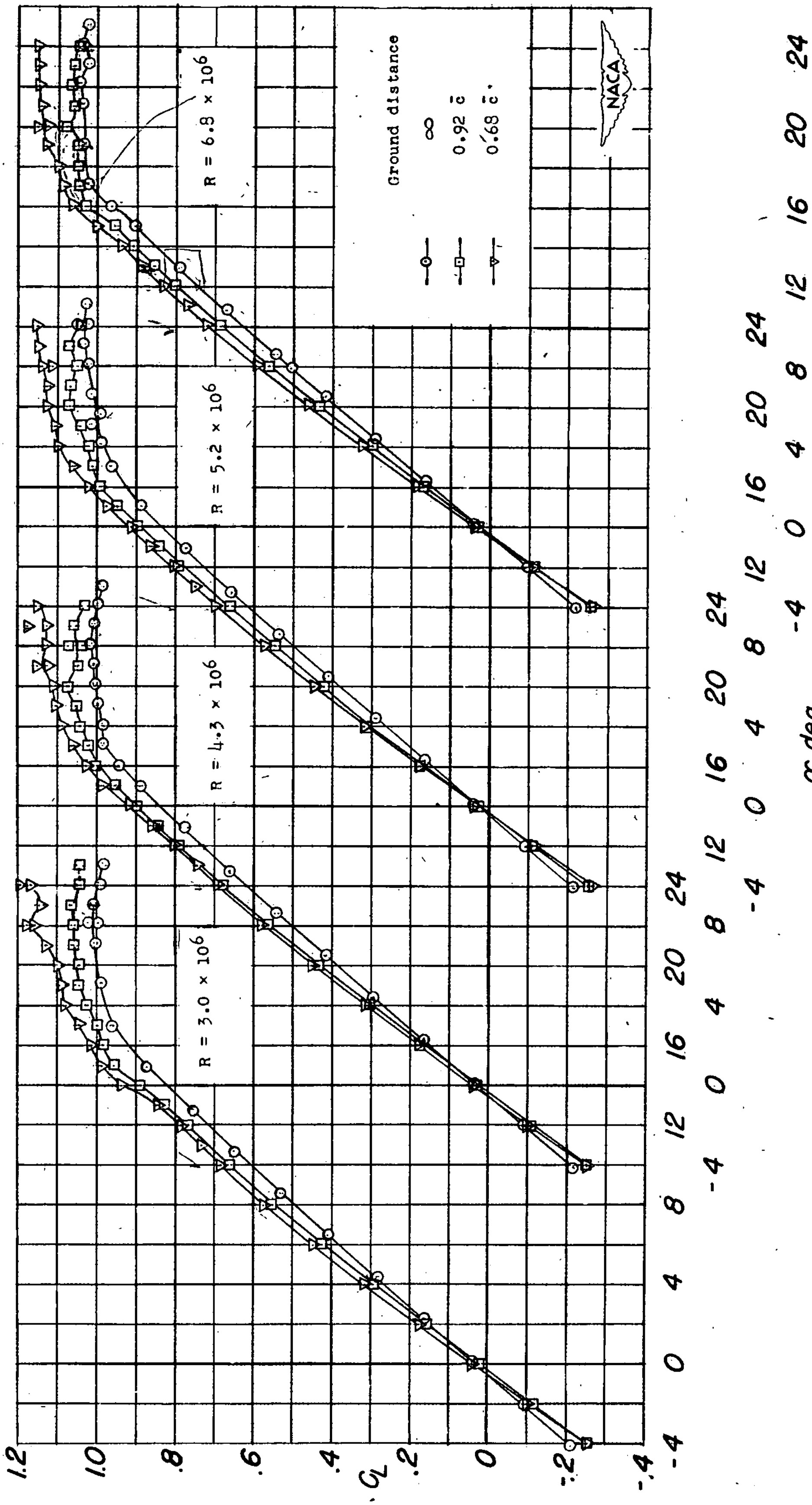

(a) Lift.

Figure 5.- Effect of ground on the aerodynamic characteristics of a 42° sweptback wing for various Reynolds numbers. Flaps neutral.

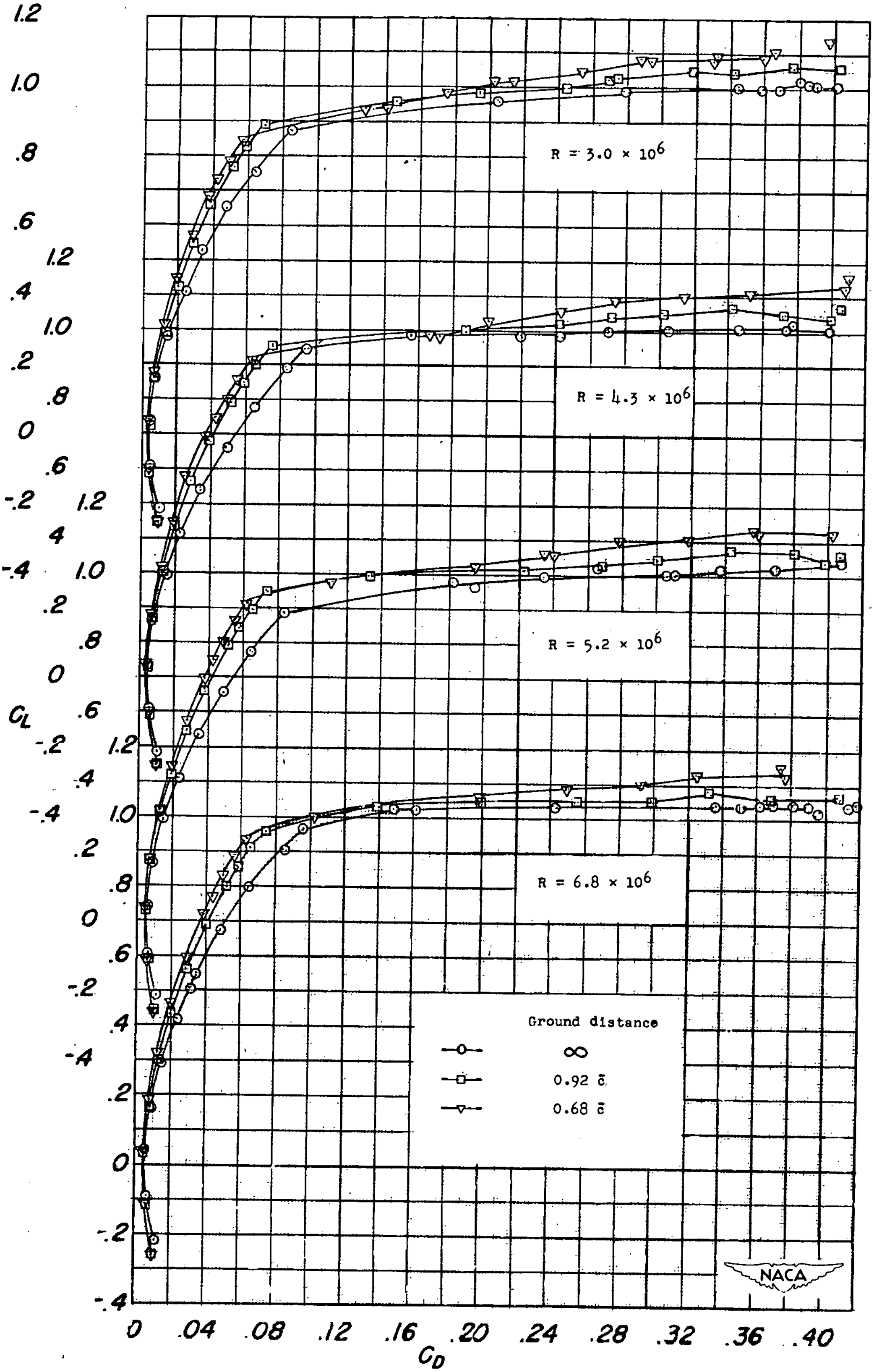

(b) Drag.

Figure 5.- Continued.

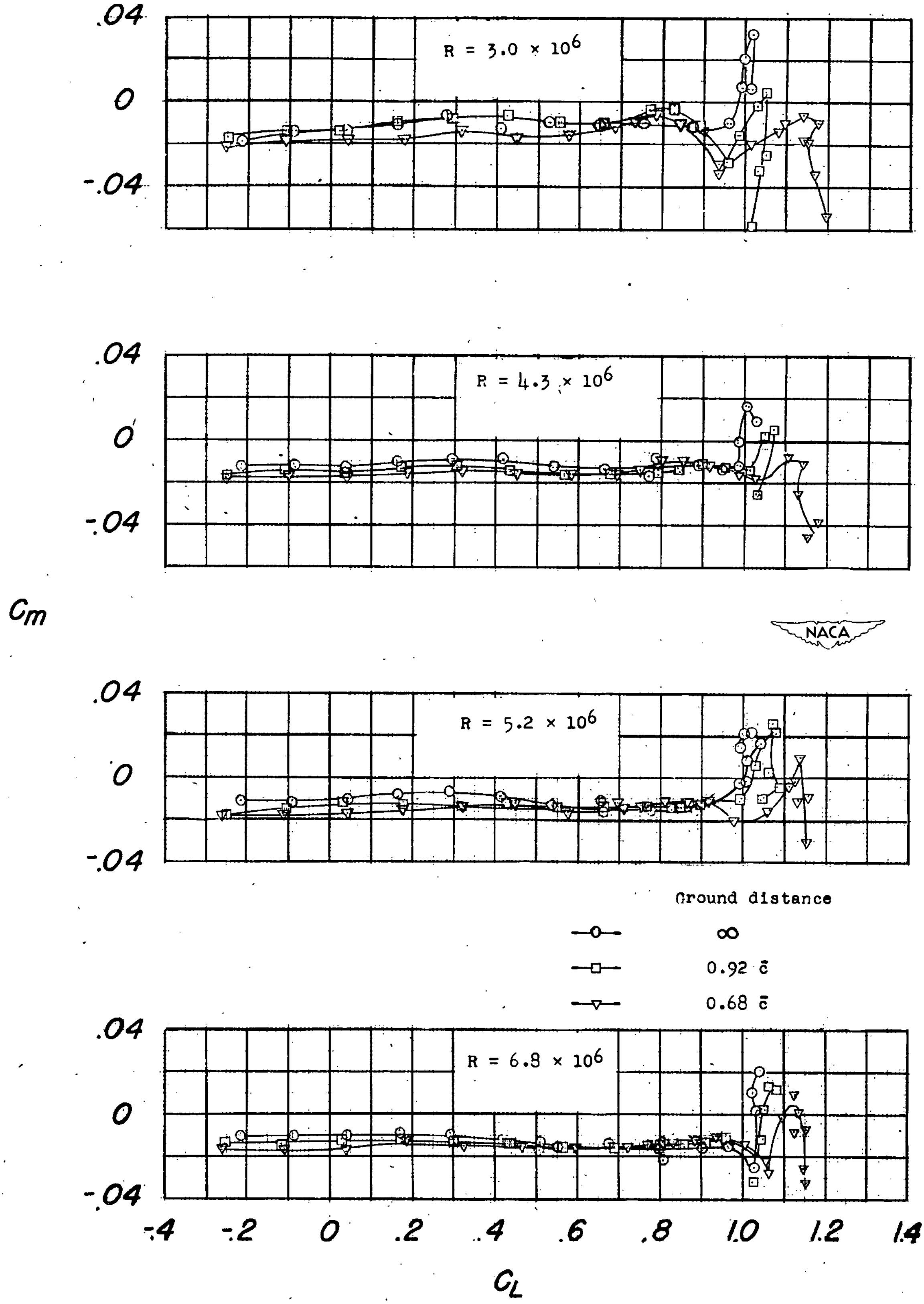

(c) Pitching moment.

Figure 5.- Concluded.

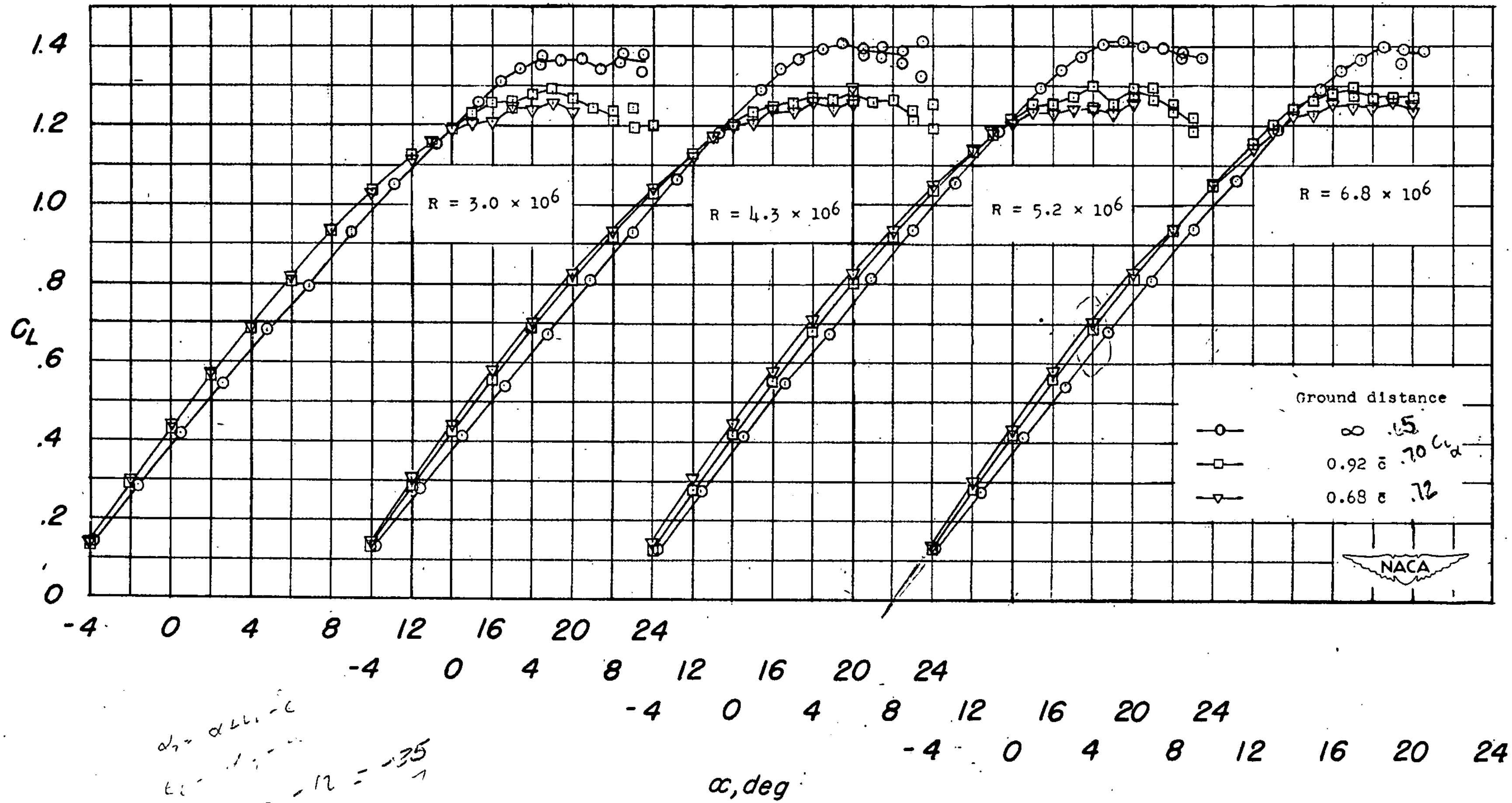

(a) Lift.

Figure 6.- Effect of ground on the aerodynamic characteristics of a 42° sweptback wing for various Reynolds numbers. Flaps deflected.

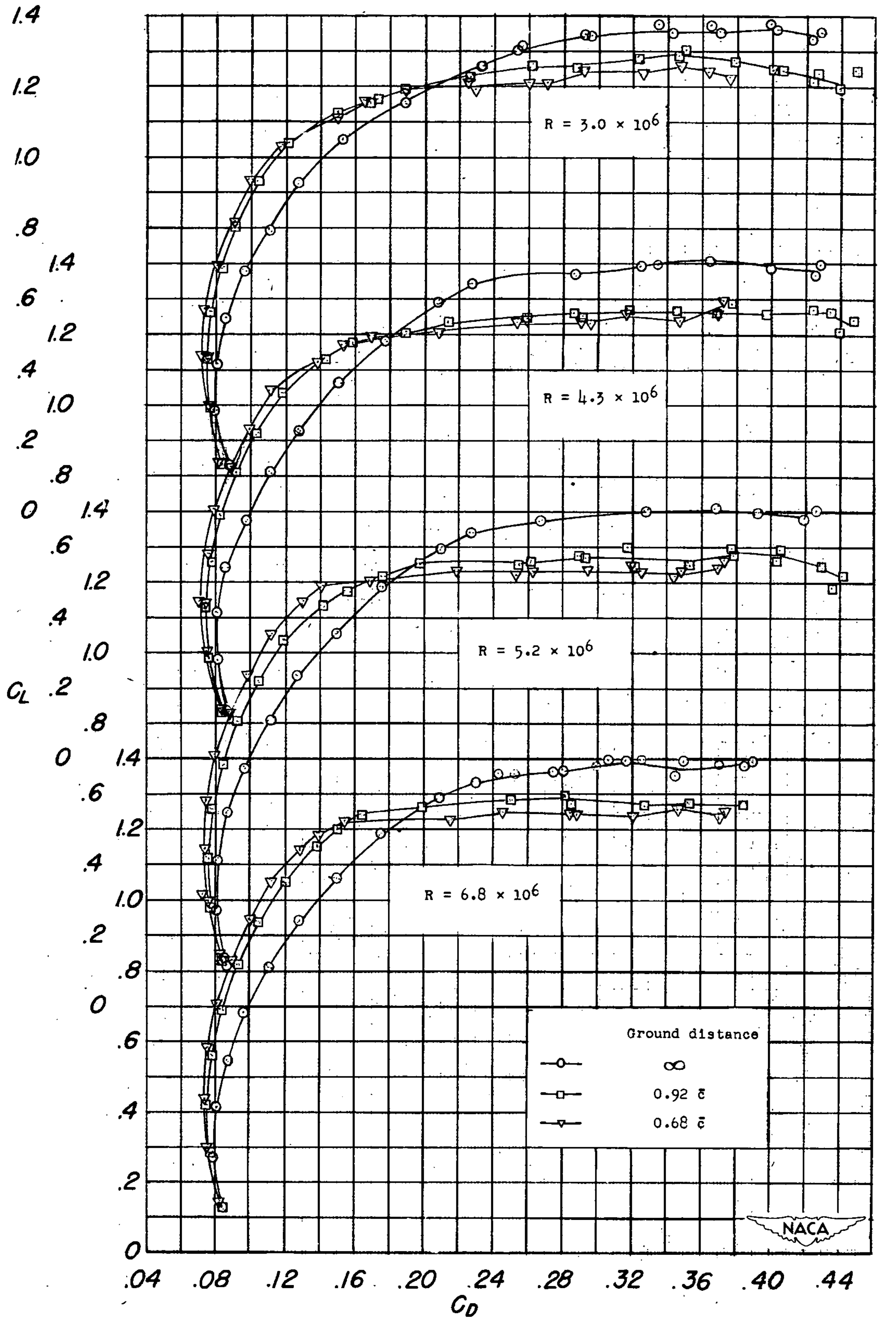

(b) Drag.

Figure 6.- Continued.

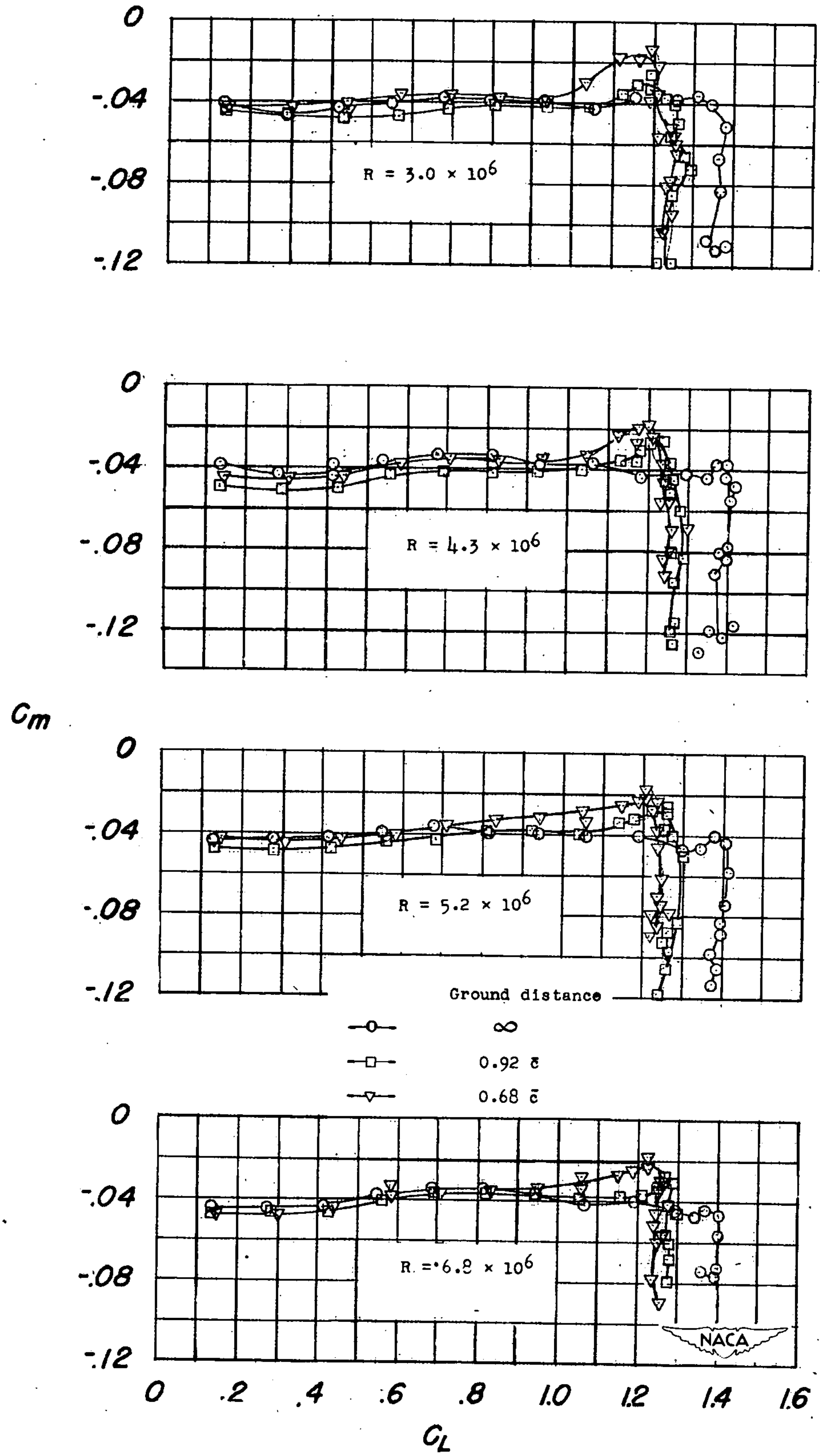

(c) Pitching moment.

Figure 6.- Concluded.

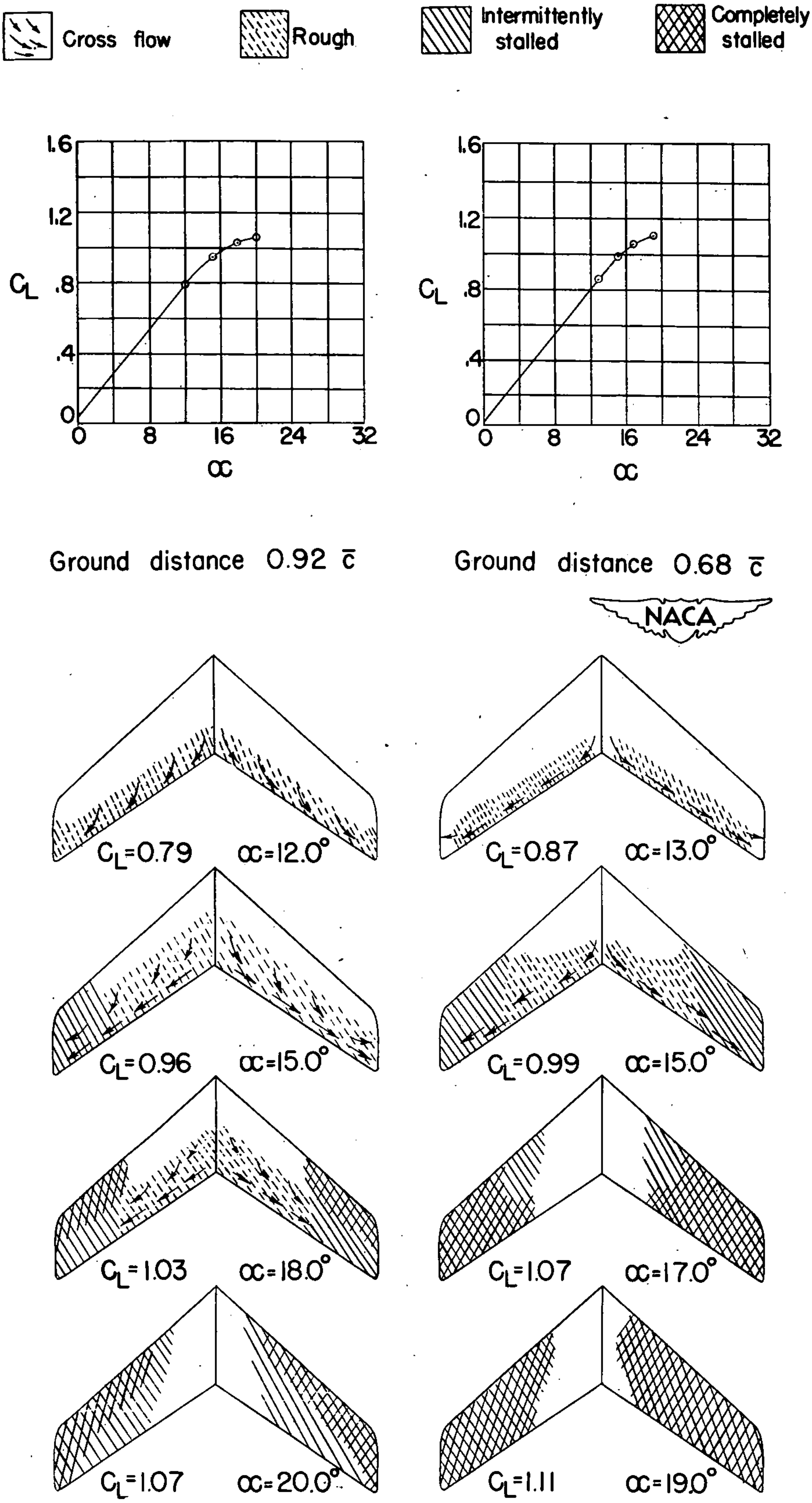

Figure 7.- Effect of ground on the stalling characteristics of a 42° sweptback wing. Reynolds number = 6.8×10^6; without flaps.

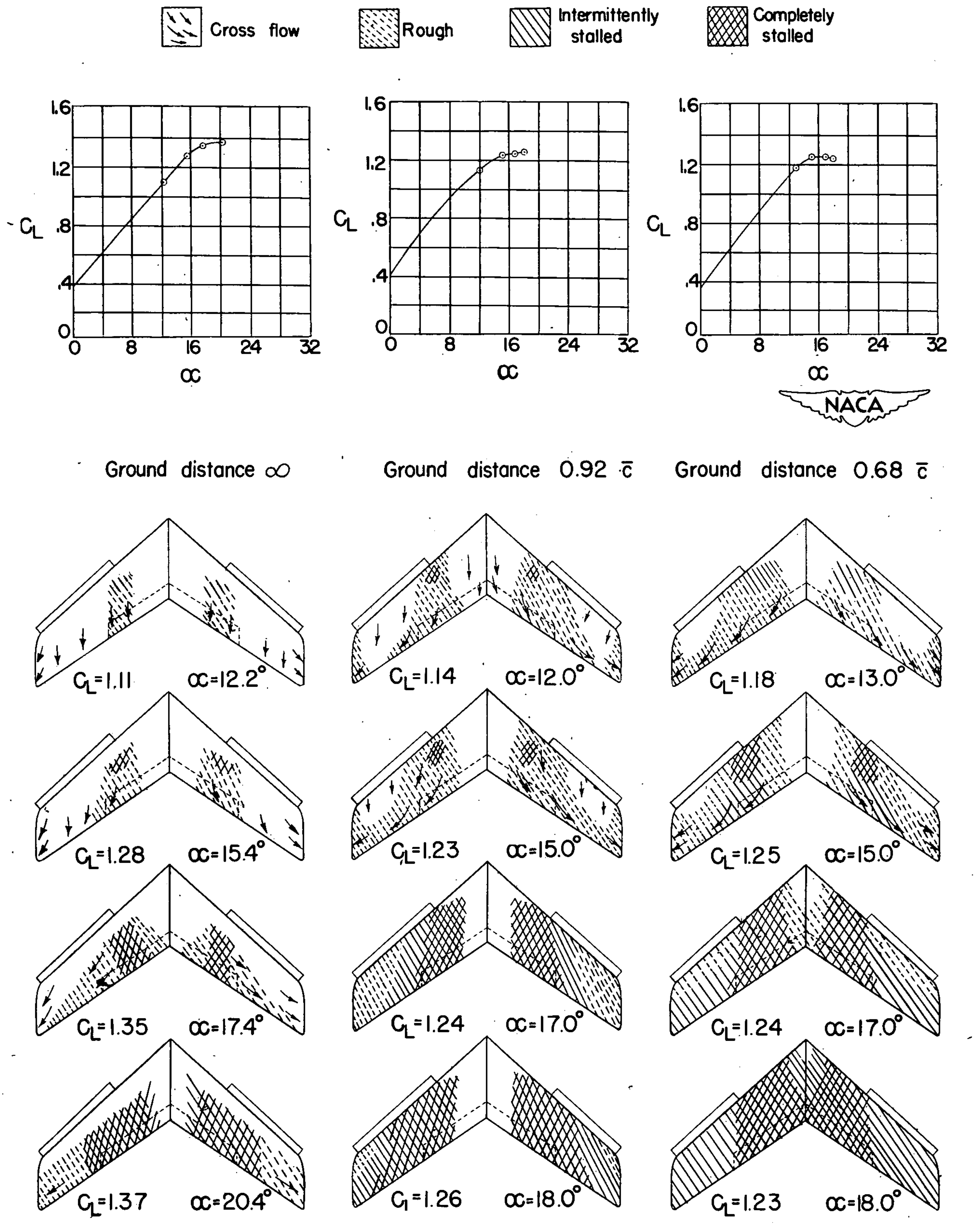

Figure 8.- Effect of ground on the stalling characteristics of a 42° sweptback wing. Reynolds number = 6.8 × 10^6; flaps deflected.